OXFORD

Cerebral Cortex, December 2020;30: 6444–6457

doi: 10.1093/cercor/bhaa206
Advance Access Publication Date: 11 August 2020
Original Article

ORIGINAL ARTICLE

Dual Role of Rbpj in the Maintenance of Neural Progenitor Cells and Neuronal Migration in Cortical Development

Alexander I. Son[1,†], Shahid Mohammad[1,†], Toru Sasaki[1], Seiji Ishii[1], Satoshi Yamashita[1], Kazue Hashimoto-Torii[1,2] and Masaaki Torii[1,2]

[1]Center for Neuroscience Research, Children's Research Institute, Children's National Hospital, Washington, DC 20010, USA and [2]Department of Pediatrics, Pharmacology and Physiology, School of Medicine and Health Sciences, The George Washington University, Washington, DC 20052, USA

Address correspondence to Kazue Hashimoto-Torii, 111 Michigan Avenue, N.W., M7633, Washington, DC 20010-2970, USA.
Email: KHashimoto-Torii@childrensnational.org; Masaaki Torii, 111 Michigan Avenue N.W., M7631, Washington, DC 20010-2970, USA.
Email: MTorii@childrensnational.org.
[†]These authors contributed equally.

Abstract

The development of the cerebral cortex is directed by a series of methodically precise events, including progenitor cell proliferation, neural differentiation, and cell positioning. Over the past decade, many studies have demonstrated the critical contributions of Notch signaling in neurogenesis, including that in the developing telencephalon. However, in vivo evidence for the role of Notch signaling in cortical development still remains limited partly due to the redundant functions of four mammalian Notch paralogues and embryonic lethality of the knockout mice. Here, we utilized the conditional deletion and in vivo gene manipulation of *Rbpj*, a transcription factor that mediates signaling by all four Notch receptors, to overcome these challenges and examined the specific roles of *Rbpj* in cortical development. We report severe structural abnormalities in the embryonic and postnatal cerebral cortex in *Rbpj* conditional knockout mice, which provide strong in vivo corroboration of previously reported functions of Notch signaling in neural development. Our results also provide evidence for a novel dual role of *Rbpj* in cell type-specific regulation of two key developmental events in the cerebral cortex: the maintenance of the undifferentiated state of neural progenitor cells, and the radial and tangential allocation of neurons, possibly through stage-dependent differential regulation of Ngn1.

Key words: cortical development, neurogenesis, neuronal migration, Notch signaling, Rbpj

Introduction

The development of the cerebral cortex with its characteristic laminar and columnar organization requires tightly coordinated sequential processes, including progenitor cell proliferation, neuronal and glial cell differentiation, cell migration, and synaptogenesis (Rubenstein and Rakic 1999; Fishell and Kriegstein 2005). One of the most important elements in cortical development is the signaling mediated by Notch receptors (Notch 1–4 in mammals), which is critically involved in many of these processes (Pierfelice et al. 2011). The binding of ligands such as Delta and Serrate (known as Jagged in mammals) to the Notch receptor results in proteolytic release of the Notch intracellular domain (NICD), which then translocates to the nucleus and binds to Rbpj (also known as Rbpjκ, Rbpsuh, or CBF1), a transcription factor and primary mediator of the canonical Notch signaling (Artavanis-Tsakonas et al. 1999; Mumm and Kopan 2000; Bray 2006). Together with its co-activators, this transcriptional complex activates downstream genes such

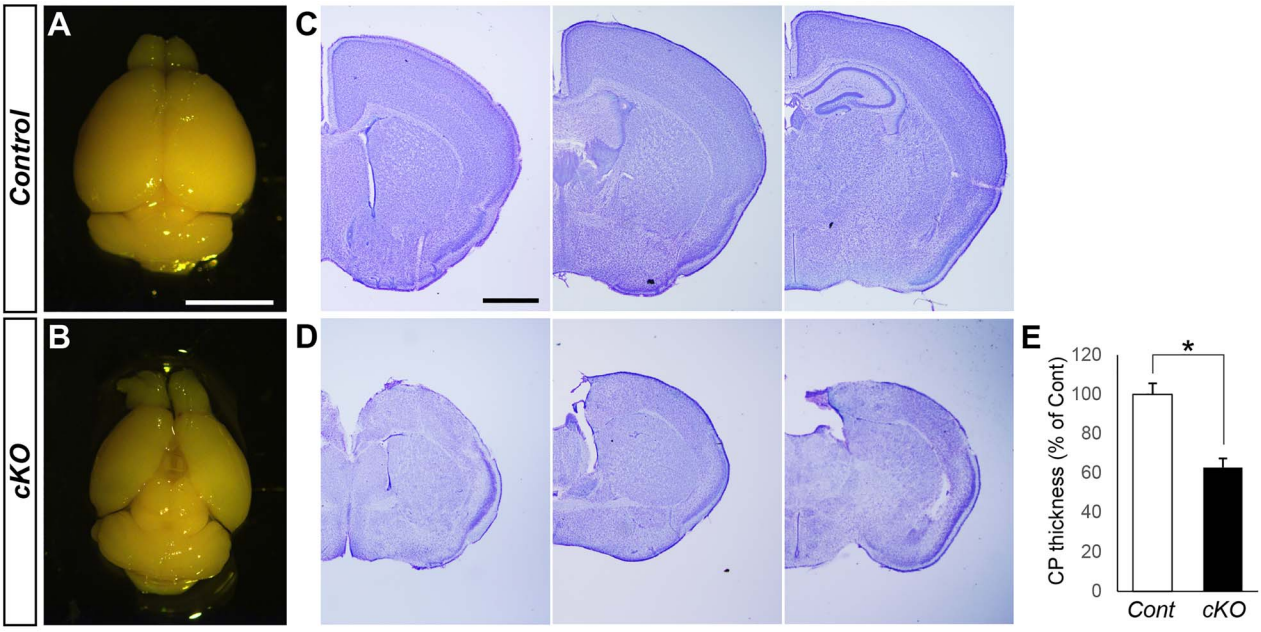

Figure 1. Smaller cerebral cortex in *Rbpj* cKO mice. (*A* and *B*) Whole brains of control (*A*) and *Rbpj* cKO (*B*) mice at P24, showing severe reduction in the size of the cortex in cKO mice. (*C* and *D*) Nissl staining of brain sections of control (*C*) and *Rbpj* cKO (*D*) mice at P24 (in the anterior to posterior order). The smaller size and lack of lamination of the cerebral cortex are apparent in the cKO brain, along with the absence of the corpus callosum and hippocampus. Bars (mm) = 5 (*A* and *B*) and 1 (*C* and *D*). (*E*) Thickness of the CP is decreased in *Rbpj* cKO mice relative to that in control mice. The data represent the mean ± standard error of the mean (SEM) ($n = 5$ animals per genotype). $^*P < 0.001$ by Student's *t*-test.

as *Hes1* and *Hes5* (Bray 2006), ultimately regulating multiple biological processes including fate specification, maintenance, and differentiation of neural stem cells and progenitor cells (Hitoshi et al. 2002; Gao et al. 2009); specification of glial cells (Taylor et al. 2007); and the survival and outgrowth of neurons, among other functions (Sestan et al. 1999; Redmond et al. 2000; Yang et al. 2004; Louvi and Artavanis-Tsakonas 2006; Mason et al. 2006; Ables et al. 2011; Imayoshi and Kageyama 2011; Pierfelice et al. 2011; Giniger 2012).

With four Notch receptors capable of potentially distinct and/or redundant functions in mammals (Andersson et al. 2011), one approach to examine the roles of canonical Notch signaling in vivo has been utilizing knockout mice of the common downstream mediator Rbpj. However, the deletion of *Rbpj* results in early embryonic lethality before the onset of neurogenesis in the nervous system (Oka et al. 1995). Thus, recent studies have utilized several lines of *Rbpj* conditional knockout (cKO) mice to examine the roles of Rbpj in various contexts during later development and in adulthood (Zhu et al. 2006; Komine et al. 2007; Taylor et al. 2007; Imayoshi et al. 2010; Liu et al. 2015). However, direct evidence for the functions of Rbpj in cortical development remains limited to those aspects during the embryonic period (Imayoshi et al. 2010; Dave et al. 2011) due likely to neonatal lethality of these mice (Nakhai et al. 2008).

Previous studies have shown the interaction between Notch signaling and Reelin-Dab1 signaling (Hashimoto-Torii et al. 2008; Keilani and Sugaya 2008; Sibbe et al. 2009; Keilani et al. 2012). This interaction mediates the Reelin signal to control the formation of radial glial scaffolds (Keilani and Sugaya 2008; Sibbe et al. 2009) and radial migration of cortical neurons (Hashimoto-Torii et al. 2008). However, the contributions of Rbpj in these processes have not been well understood, and it remains unknown whether Notch-Rbpj signaling deficit leads to other characteristic *reeler* phenotypes such as radial glial dysmorphology (Dulabon et al. 2000; Forster et al. 2002; Hartfuss et al. 2003), neuronal invasion into layer I (Trommsdorff et al. 1999; Hack et al. 2007) and disrupted cortical lamination (Caviness and Sidman 1973).

In this study, we examined the role of Rbpj in cortical development using cortex-specific *Rbpj* cKO mice and *in utero* electroporation (EP)-mediated gene manipulation approaches. Our results demonstrate that Rbpj plays two critical cell type-specific roles in cortical development. First, Rbpj is an essential player for the maintenance of neural progenitor cells for controlled neurogenesis by inhibiting their premature differentiation into neurons. Second, Rbpj is required for the proper radial and tangential positioning of cortical neurons through the preservation of radial glial scaffolds and cell-autonomous regulation of neuronal migration. Our results also suggest the involvement of opposite regulations of Neurogenin1 (Ngn1) by Rbpj in neural progenitor cells and migrating neurons in these processes. Together, our work demonstrates the multimodal and complex function of Rbpj in cortical development.

Materials and Methods

Mice

All animals were handled according to protocols approved by the Institutional Animal Care and Use Committees of the Children's National Hospital. Generation and genotyping of the floxed *Rbpj* mouse line (provided by T. Honjo) has been described previously (Han et al. 2002; Tanigaki et al. 2002). Cerebral cortex-specific *Rbpj* cKO mice were generated by crossing floxed *Rbpj* mice with *Emx1-Cre* mice (Jackson lab) and kept under a C57/BL6J background. Although homozygous *Rbpj* cKO mice (*Emx1-Cre;Rbpj*$^{fl/fl}$)

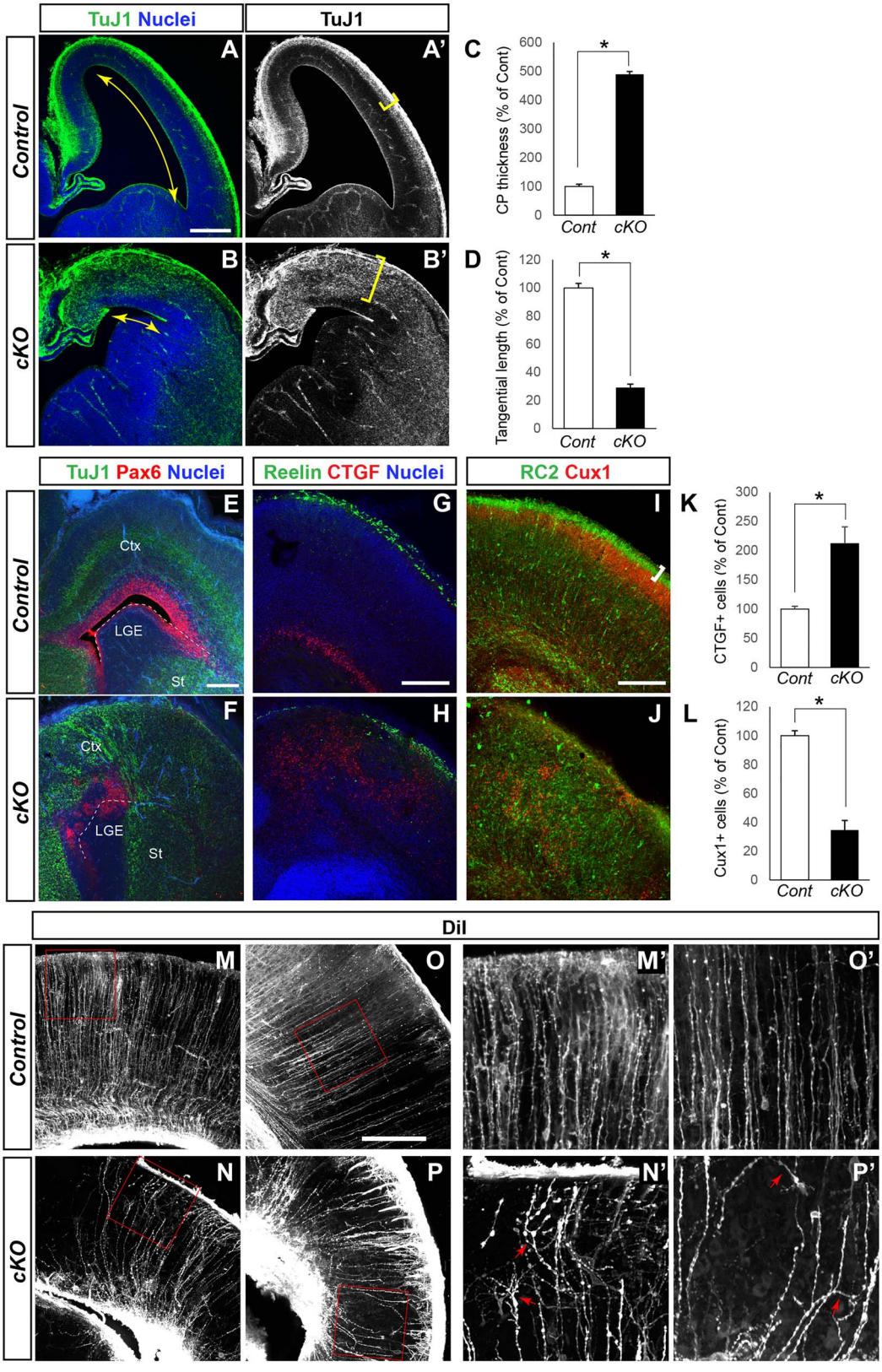

Figure 2. Premature neurogenesis and disrupted radial glial structure in the cortex of *Rbpj* cKO mice. (*A*–*B*′) Immunohistochemistry for TuJ1 at E15.5, showing the thicker CP occupied by TuJ1^{+} neurons (brackets) and smaller tangential length of the ventricular surface (arrows) in cKO mice (*B* and *B*′) comparing with those in control mice

survive until adulthood [at least until postnatal day (P) 50], these mice experience hair loss followed by cyst formation throughout the body as early as a few days after birth, which becomes more severe with age. As such, our examination of these mice was mostly done by adolescence (P35). Conditional heterozygous *Emx1-Cre;Rbpj*$^{fl/+}$ mice were used as the control. CD-1 mice (The Jackson Laboratory) were used for EP experiments.

Constructs and in utero Electroporation

In utero EP was carried out at E13.5 or E14.5 as previously described (Torii and Levitt 2005; Hashimoto-Torii et al. 2008) with the following constructs: pTα1-Cre-IRES-Venus (4 mg/mL) (Hashimoto-Torii et al. 2008), pCMX and pCMX-dominant negative mouse Rbpj (R218H, 4 mg/mL) (Kato et al. 1997), pCAG-DsRed2 and pCAG-EGFP (Hashimoto-Torii et al. 2003; Torii and Levitt 2005) (0.5 mg/mL), and Hes1p-dVenus, Hes1pAmBm-dVenus and TP-1-dVenus, rBG-dVenus (Kohyama et al. 2005) (4 mg/mL, gifts from H. Okano).

Immunohistochemistry

Brains were fixed with 4% paraformaldehyde in phosphate-buffered saline overnight. A total of 40–70 µm-thick coronal vibratome slices or 18 µm coronal cryosections were collected. The following primary antibodies were used; polyclonal anti-GFP (also detect Venus and dVenus; 1:200; Abcam), anti-DsRed (1:5000; BD Biosciences), anti-BrdU (1:100; Accurate), anti-CTGF (1:500; Abcam), anti-Cux1 (1:300; Santa Cruz Biotechnology), anti-FoxP2 (1:10000; Abcam), anti-Pax6 (1:500; Covance), anti-Rbpj (1:100; Cell Signaling), monoclonal anti-Reelin (1:2000; Chemicon), anti-RC2 (1:5; Developmental Studies Hybridoma Bank), anti-Crym (1:500; Abcam), anti-Ki67 (1:200; Vector), anti-Ngn1 (1:500; a kind gift from J.E. Johnson), and anti-β tubulin (class III) (TuJ1; 1:200; Covance) antibodies. Immunohistochemistry was performed as described previously (Hashimoto-Torii et al. 2003; Torii and Levitt 2005; Torii et al. 2009). For the amplification of dVenus detection, the TSA Plus Fluorescein system (PerkinElmer) was used. The slices and sections were nuclear counterstained with TO-PRO3 or DAPI (Molecular Probes). For TUNEL staining, the ApopTag kit (Chemicon) was used. Images were acquired using the LSM510 (Carl Zeiss) or Olympus FV1200 confocal microscope.

DiI Labeling

To label radial glia, saturated DiI solution (in ethanol) was injected into the lateral ventricle of P0 brains fixed with 4% paraformaldehyde. After 48 h of incubation at 37°C, coronal vibratome slices were made at 100 µm thickness and photographed using an Olympus FV1200 confocal microscope.

Quantitative Analyses

For all analyses, investigators were blind to the genotype and experimental conditions. Measurements were performed focusing at the level of the somatosensory cortex, as all the phenotypes were consistent across the entire anterior–posterior levels. Tangential length of the cortex was measured as the distance from the cortex-ganglionic eminence boundary to the cortex-(presumptive) hippocampal primordium boundary along the ventricular surface, and the thickness of cortical plate (CP) was measured at the center of this tangential span of the cortex. The relative values were then calculated against the average values for the control mice set as 100. For the quantification of layer-specific neuronal subtypes, the number of marker-positive neurons per cortical column of 100 µm width was calculated for each sample, and normalized against the average value for the control mice set as 100. The number of Ki67$^+$, Ki67$^-$, Ngn1$^+$, DsRed2$^+$, dVenus$^+$, EGFP$^+$ single- or double-labeled cells was similarly counted, and the percentage against the number of DsRed2$^+$, dVenus$^+$, Ngn1$^+$ or DAPI$^+$ cells was calculated. To quantify the radial distribution of neurons, the cortex was radially divided into 10 equal-sized bins from the ventricle to the pia. The cells in each bin were quantified and normalized as the percentage of total cells counted. For the analysis of neuronal morphology, neurons located in the lower CP close to the intermediate zone (IZ) were analyzed. Axons and the endfeet attaching to the marginal zone were excluded in our quantification of the number of the primary processes and the number of branching points, respectively. For the cell cycle exit analysis, we followed previous studies (Chenn and Walsh 2002; Sanada and Tsai 2005). Bromodeoxyuridine (BrdU, at 50 mg/kg body weight) was injected 24 h after the EP at E14.5, and the brains were fixed after another 24 h.

Results

Absence of *Rbpj* in the Developing Cerebral Cortex Accelerates Neurogenesis and Prematurely Depletes Neural Progenitor Cells

To examine the effects of *Rbpj* deficiency in the developing cerebral cortex, we generated cortex-specific *Rbpj* cKO mice by crossing floxed *Rbpj* mice (Han et al. 2002; Tanigaki et al. 2002)

(*A* and *A*′). Nuclei were counterstained with DAPI in *A* and *B*. Bar (µm) = 200. (*C* and *D*) The quantification of the tangential length of the ventricular surface (*C*) and thickness of the CP (*D*). The data represent the mean ± SEM relative to the mean value of control mice ($n = 5$ animals per genotype). *$P < 0.001$ by Student's *t*-test. (*E* and *F*) Immunohistochemistry for TuJ1 and Pax6 in control (*E*) and cKO (*F*) cortices at P0, showing premature depletion of Pax6$^+$ neural progenitor cells in the VZ of cKO mice. Nuclei were counterstained with DAPI. Dotted lines trace the ventricular surface of the LGE. Bar (µm) = 200. (*G* and *H*) Immunohistochemical labeling of Reelin$^+$ Cajal-Retzius cells and CTGF$^+$ subplate neurons in control (*G*) and cKO (*H*) cortices at P0. Reelin$^+$ neurons in control and cKO cortices show similar layer I-specific distribution, whereas normally laminar-specific distribution of CTGF$^+$ neurons (*G*) is highly disrupted in the cKO cortex (*H*). Nuclei were counterstained with DAPI. Bar (µm) = 200. (*I* and *J*) Immunohistochemistry for RC2 and Cux1 in control (*I*) and cKO (*J*) cortices at P0. The laminar-specific distribution of Cux1$^+$ upper layer neurons (*I*) is disrupted in cKO mice (*J*). RC2 staining reveals that comparing with uniform distribution of radial glial fibers that show clear accumulation of their endfeet at the pial surface of the cortex in control mice (*I*, bracket), the cKO cortex exhibits their irregular distribution and lack of endfeet accumulation at the pial surface (*J*). Bar (µm) = 200. (*K* and *L*) A number of CTGF$^+$ (*K*) and Cux1$^+$ neurons (*L*) per unit width of the cortex. The data represent the mean ± SEM relative to the mean value of control mice ($n = 5$ animals per genotype). *$P < 0.05$ (*K*) and *$P < 0.001$ (*L*) by Student's *t*-test. (*M*–*P*′) DiI-labeled radial glial fibers in control (*M*, *M*′, *O* and *O*′) and cKO (*N*, *N*′, *P* and *P*′) cortices at P0. *M*, *N*, and *O*, *P* show the medial and lateral part of the cortex, respectively. *M*′, *N*′, *O*′, and *P*′ are higher magnification view of the boxed areas in *M*, *N*, *O*, and *P*, respectively. Compared with the straight and evenly distributed fibers reaching to the pial surface in control, many fibers are curved and/or branched before reaching to the pia (arrows) in cKO mice. *Ctx*, cortex; LGE, lateral ganglionic eminence; St, striatum.

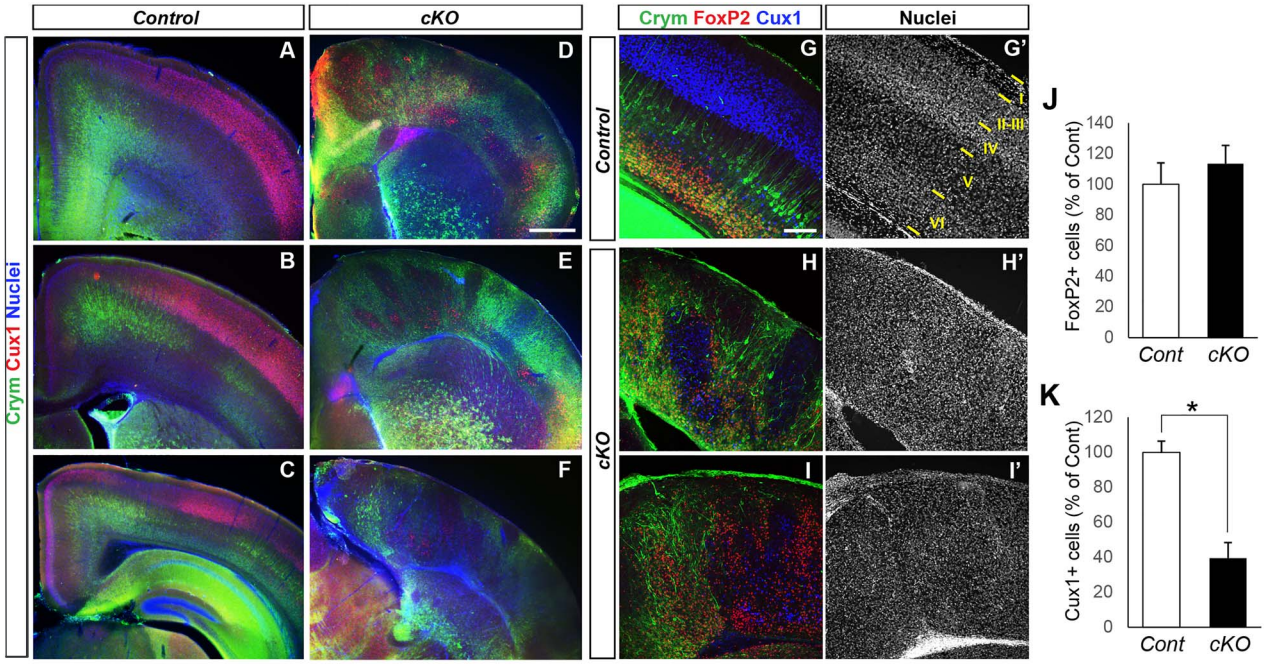

Figure 3. Disruption of the laminar organization of the cortex in *Rbpj* cKO mice. (*A–F*) Immunohistochemistry for layer-specific neuronal markers in the cortex of control (*A–C*) and cKO (*D–F*) mice at P14 (in the anterior to posterior order). Nuclei were counterstained with DAPI. Laminar-specific distribution of Cux1$^+$ upper-layer neurons and Crym$^+$ lower-layer neurons (*A–C*) is severely disrupted, forming discrete clustering patterns throughout the entire cortex in cKO mice (*D–F*). Relative increase of lower-layer neurons and decrease of upper-layer neurons in the cKO cortex are also observed. Bar (μm) = 500. (*G–I′*) The cortex labeled for Crym$^+$, FoxP2$^+$ and Cux1$^+$ layer-specific neuronal subtypes (*G–I*) and TO-PRO3 nuclear staining (*G′–I′*) at P34. Compared with the clear laminar pattern in the distribution of neuronal subtypes and cell densities observed in the control (*G* and *G′*), the cKO cortex show the lack of laminar pattern (*H–I′*). Bars (μm) = 200. (*J* and *K*) Number of FoxP2$^+$ (*J*) and Cux1$^+$ neurons (*K*) per unit width of the cortex. The data represent the mean ± SEM relative to the mean value of control mice ($n = 6$ animals per genotype). $P = 0.49$ (*J*) and $^*P < 0.01$ (*K*) by Student's *t*-test.

with *Emx1-Cre* mice (The Jackson Laboratory) (Fig. 1). In these cKO (*Emx1-Cre;Rbpj*$^{fl/fl}$) mice, *Rbpj* is deleted in all cells originated from cortical neural progenitor cells (Supplementary Fig. 1). Heterozygous *Emx1-Cre;Rbpj*$^{fl/+}$ mice were used as the control.

In comparison to controls, the cortex size in cKO mice was significantly smaller at postnatal day (P) 24 (Fig. 1). Although brain regions that are connected with the cortex such as thalamus also showed reduction in size in cKO mice, most other parts such as the cerebellum and midbrain appeared grossly normal (Fig. 1A–D), consistent with the cortex-specific deletion of *Rbpj*. In addition, the absence of the hippocampus, corpus callosum, and cortical laminar organization was observed in cKO brains (Fig. 1D).

The role of Rbpj in the maintenance of cortical neural stem cells in the embryonic brain has been previously demonstrated using other cKO lines (*Nestin-Cre;Rbpj*$^{fl/fl}$ and *Nestin-CreERT2;Rbpj*$^{fl/fl}$) (Imayoshi et al. 2010; Dave et al. 2011) and ribonucleic acid interference (RNAi)-mediated knockdown (Mizutani et al. 2007). Given that the smaller cortex is likely attributed to defects in the maintenance of neural stem/progenitor cells, we first examined the degree of cortical neurogenesis in our cKO mice (Fig. 2). Immunohistochemistry for the neuronal marker TuJ1 at embryonic day (E) 15.5 showed that CP was thicker in cKO mice compared with controls (Fig. 2A–C), whereas the tangential length of the ventricular surface that consists of neural progenitor cells was significantly smaller in cKO mice (Fig. 2B, B′, D). These results suggest that neural progenitor cells are prematurely differentiated into neurons and depleted in the cortex of cKO mice.

Consistent with these observations, the labeling for Pax6 at P0 demonstrated a severe reduction of neural progenitor cells according to the decreased tangential size of the ventricular zone (VZ) in the cKO cortex (Fig. 2E, F). In the CP, the number of CTGF$^+$ subset of subplate neurons generated from the cortical neural progenitor cells at the earliest period of neurogenesis per unit width (per column) was higher in the cKO cortex than that in the control at P0 (Fig. 2G, H, K). Severe disruptions in their laminar distribution in cKO mice were also observed (Fig. 2H). The Reelin$^+$ Cajal-Retzius cells, which are also among the earliest-generated neuronal population, appeared to be less evenly distributed in cKO mice comparing with those in controls, but still localized on the surface of the cortex (Fig. 2G, H), consistent with their origin outside of the cortex (Corbin et al. 2001). In contrast to these early-generated neurons, the number of Cux1$^+$ neurons that are generated from the cortical progenitors during late embryonic stages was much smaller in the cKO cortex compared with that in controls (Fig. 2I, J, L), consistent with the premature depletion of neural progenitor cells. These Cux1$^+$ neurons also showed severe disruption in distribution in cKO mice in contrast to the continuous distribution specific in upper cortical layers (layers II-IV) in control mice (Fig. 2I, J).

Given the abnormal distribution patterns of CTGF$^+$ and Cux1$^+$ neurons generated from cortical progenitor cells, we examined the organization of radial glial processes, which serve as essential scaffolds for the radial migration of cortical neurons (Rakic 2003, 2007). Immunohistochemistry with the radial glial cell Marker-2 antibody (clone RC2) and DiI (1,1′-dioctadecyl-3,3,3′,3′-tetramethylindocarbocyanine perchlorate)

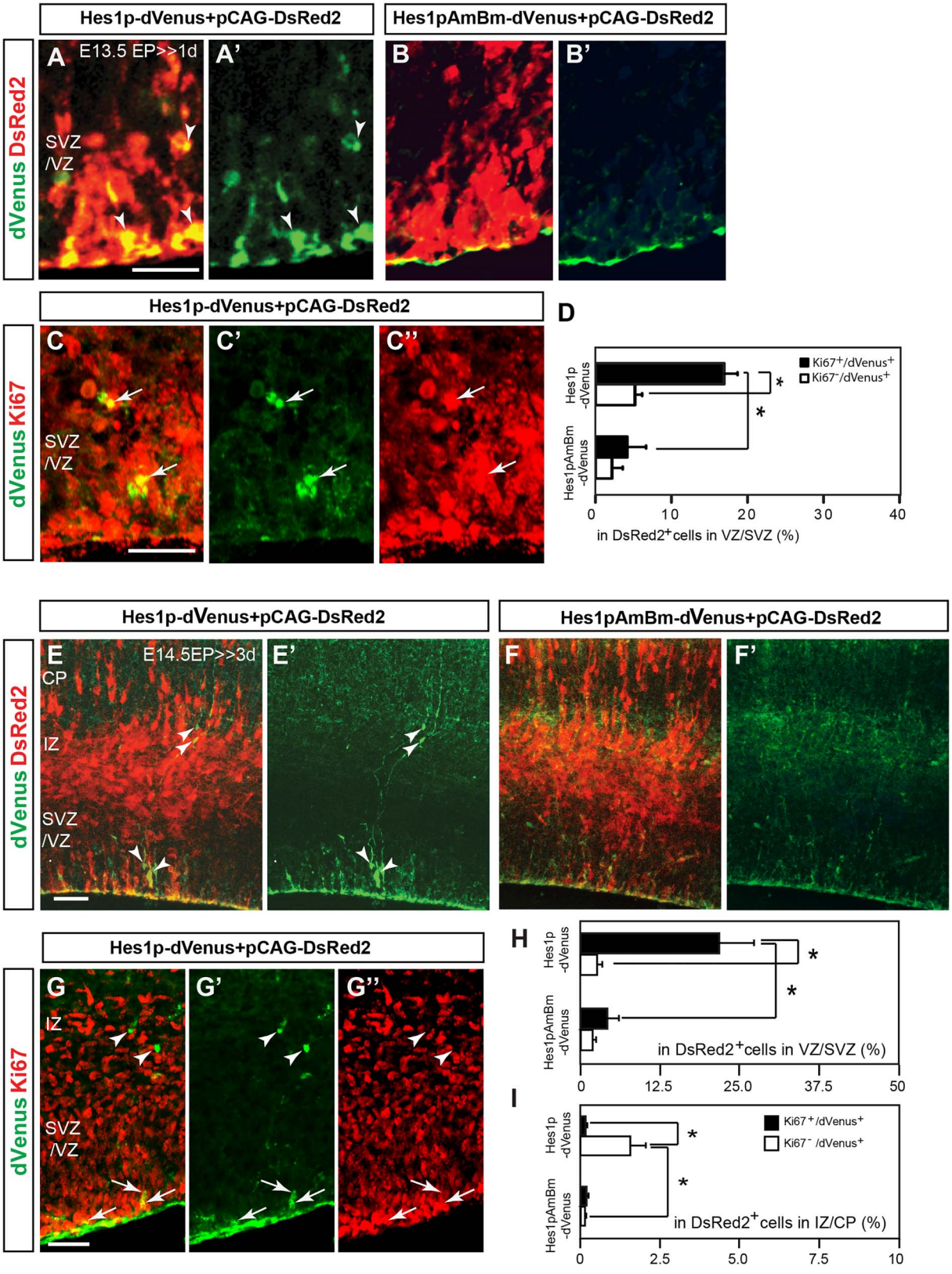

Figure 4. Pattern of Rbpj transcriptional activity during cerebral cortical development. (A–B′) Immunostaining for dVenus and DsRed2 1 day after EP at E13.5 with indicated plasmids. dVenus expression driven by the Hes1 promoter is observed in neural progenitor cells in the VZ/subventricular zone (SVZ) (arrowheads in A and A′).

labeling of radial glia revealed that, in association with the premature depletion of neural progenitor cells and accelerated neurogenesis, radial glial fibers in cKO mice were not evenly distributed along the tangential axis of the cortex (Fig. 2J, N, N′, P, P′) in contrast to the even distribution in control mice (Fig. 2I, M, M′, O, O′). In addition, in contrast to the radially elongated shape of radial glial fibers with their endfeet accumulated at the pial surface observed in controls (Fig. 2I, M′), most radial glial fibers in cKO mice are curved or branched, and do not reach the pial surface (Fig. 2J, N′), suggesting that their abnormal shape may also contribute to the incorrect positioning of cortical neurons.

Rbpj is Required for Proper Radial and Tangential Positioning of Cortical Neuronal Subtypes

Based on our observation, we further examined the organization of the cortex at later postnatal ages using molecular markers for layer-specific neuronal subtypes (Fig. 3). Immunohistochemical labeling at P14 and P34 showed that each of the neuronal subtypes is generated in the *Rbpj* cKO cortex. However, instead of positioning into specific cortical layers that are continuous along the tangential axis of the cortex in the normal cortex (Fig. 3A–C), the distribution of these neuronal subtypes was severely disorganized throughout the cortex along both the radial and tangential axes in cKO mice (Fig. 3D–F). Cux1$^+$ (layers II–IV) neurons formed segregated clusters surrounded by Crym$^+$ (layers V and VI) neurons, whereas FoxP2$^+$ (layer VI) neurons often intermingled with Cux1$^+$ neurons and Crym$^+$ neurons (Fig. G and H). In some cases, Cux1$^+$ neurons and Crym$^+$ neurons, which normally form distinct cortical layers, were segregated into tangential domains (Fig. 3G, I). The number of Cux1$^+$ per unit width (per column) of the cortex was greatly reduced in the cKO cortex compared with controls (Fig. 3K) similar to the observation at P0 (Fig. 2), whereas the number of FoxP2$^+$ neurons per unit width was comparable with that in controls (Fig. 3J). Consistent with abnormal distribution of neuronal subtypes, the laminar variation of cell packing density observed in the cortex of control mice was lost in cKO mice (Fig. 3G′–I′). The marginal zone (layer I), which normally is a relatively cell-poor layer, was also fully invaded by cortical neurons in the cKO cortex (Fig. 3G′–I′).

These results demonstrate that the cKO cortex undergoes accelerated neurogenesis and premature depletion of neural progenitor cells, as well as abnormal morphology of radial glial fibers (Fig. 2). Together, these abnormalities likely lead to the formation of a smaller cerebral cortex with a relatively larger number (per unit width of the cortex) of early-born lower-layer neurons and smaller number (per unit width of the cortex) of later-born upper-layer neurons, both of which show severe radial and tangential positioning defects (Fig. 3).

Transcriptional Function of Rbpj is Activated in the Progenitor Cells and Migrating Neurons

The cortical phenotype in cKO mice suggested that Rbpj plays essential roles in both neural progenitor cells and neurons. We have previously examined Rbpj activity using the TP-1-dVenus construct, which expresses dVenus, a Venus variant yellow fluorescent protein that is fused with the PEST domain for accelerated degradation [e.g., reduces the half-life of Enhanced Green Fluorescent Protein (EGFP) from ~26 h to ~2 h in mammalian cells) (Li et al. 1998)], under the control of a minimal promoter and the Rbpj binding motifs (Kato et al. 1997; Hashimoto-Torii et al. 2008). Here, we further examined the pattern of the transcriptional activity of Rbpj in the developing cortex using an additional reporter construct, Hes1p-dVenus, which contains the promoter of *Hes1*, a downstream target of Rbpj (Kohyama et al. 2005) (Fig. 4). The Hes1p-dVenus plasmid was introduced into the wild-type mouse cerebral cortex at E13.5 using in utero EP, together with the pCAG-DsRed2 plasmid for the labeling of electroporated cells (Hashimoto-Torii et al. 2008), and brains were observed 24 h later. dVenus$^+$ cells were detected by immunohistochemistry in a subset of DsRed2$^+$ cells in the VZ, mostly in mitotic (Ki67$^+$) neural progenitor cells (Fig. 4A, A′, C–D). When the Hes1p-dVenus and pCAG-DsRed2 plasmids were introduced at E14.5 and brains were observed 3 days later, dVenus$^+$ cells were detected in both mitotic (Ki67$^+$) neural progenitor cells in the VZ with characteristic elongated radial fibers, as well as in postmitotic (Ki67$^-$) neurons in the IZ (Fig. 4E, E′, G–I). Very few dVenus$^+$ cells were found in Ki67$^-$ cells within the VZ (Fig. 4G–H). Similar results were obtained using the TP-1-dVenus plasmid (Supplementary Fig. 2). Control EPs with the Hes1pAmBm-dVenus (in which the Hes1 promoter was mutated in its Rbpj binding sites) (Kohyama et al. 2005) or rBG-dVenus (in which Rbpj binding sites were deleted from the minimum promoter of TP-1) resulted in very few Venus$^+$ cells (Fig. 4B, B′, D, F, F′, H, I, Supplementary Fig. 2). These observations suggest that Rbpj activity is tightly dependent on the developmental state of cortical cells: active in neural progenitor cells, acutely turned off in newly-generated neurons and turned on again in neurons upon migration.

Rbpj is Required for the Maintenance of Neural Progenitor Cells in the Developing Cortex

The severe cortical phenotype in the cKO likely exhibits a mixture of primary and secondary impacts of *Rbpj* deletion in neural progenitor cells and neurons. To decipher the cell-autonomous roles of Rbpj activated in neural progenitor cells and migrating neurons, we next examined the effect of Rbpj manipulation using in utero EP. We co-introduced a plasmid that expresses a dominant-negative form of Rbpj (dnRbpj) (Kato et al. 1997) under the ubiquitous cytomegalovirus promoter (Kolk et al.

Little dVenus expression was induced by the control Hes1pAmBm promoter (B and B′). The signal at the apical surface in dVenus staining is nonspecific signal introduced during the process of amplified detection of weak dVenus expression. Bar (μm) = 50. (C–C″) Immunostaining for dVenus and Ki67 1 day post-EP at E13.5 with Hes1p-dVenus showing the expression of dVenus mainly in Ki67$^+$ mitotic neural progenitor cells in the VZ/SVZ (arrows). Bar (μm) = 50. (D) Percentages of Ki67$^+$/dVenus$^+$ (black bars) and Ki67$^-$/dVenus$^+$ (white bars) cells in the VZ/SVZ in the DsRed2$^+$ cells electroporated with indicated plasmids. The data represent the mean ± SEM (n = 6 animals per condition). *P < 0.001 by Student's t-test. (E–F′) Immunostaining for dVenus and DsRed2 3 days after EP at E14.5 with indicated plasmids. dVenus expression driven by Hes1 promoter is observed in both neural progenitor cells in the VZ and migrating neurons in the IZ (arrowheads in E and E′). Little dVenus expression was induced by Hes1pAmBm-dVenus (F and F′). Bar (μm) = 50. (G–G″) Immunostaining for dVenus and Ki67 3 days post-EP at E14.5 with Hes1p-dVenus, showing the expression of dVenus mainly in Ki67$^+$ mitotic neural progenitor cells in the VZ (arrows) and Ki67$^-$ neurons in the IZ (arrowheads). Bar (μm) = 50. (H and I) Percentages of Ki67$^+$/dVenus$^+$ (black bars) and Ki67$^-$/dVenus$^+$ (white bars) cells in DsRed2$^+$ cells electroporated with indicated plasmids in the VZ/SVZ (top) or IZ/CP (bottom). The data represent the mean ± SEM (n = 6 animals per condition). *P < 0.01 by Student's t-test.

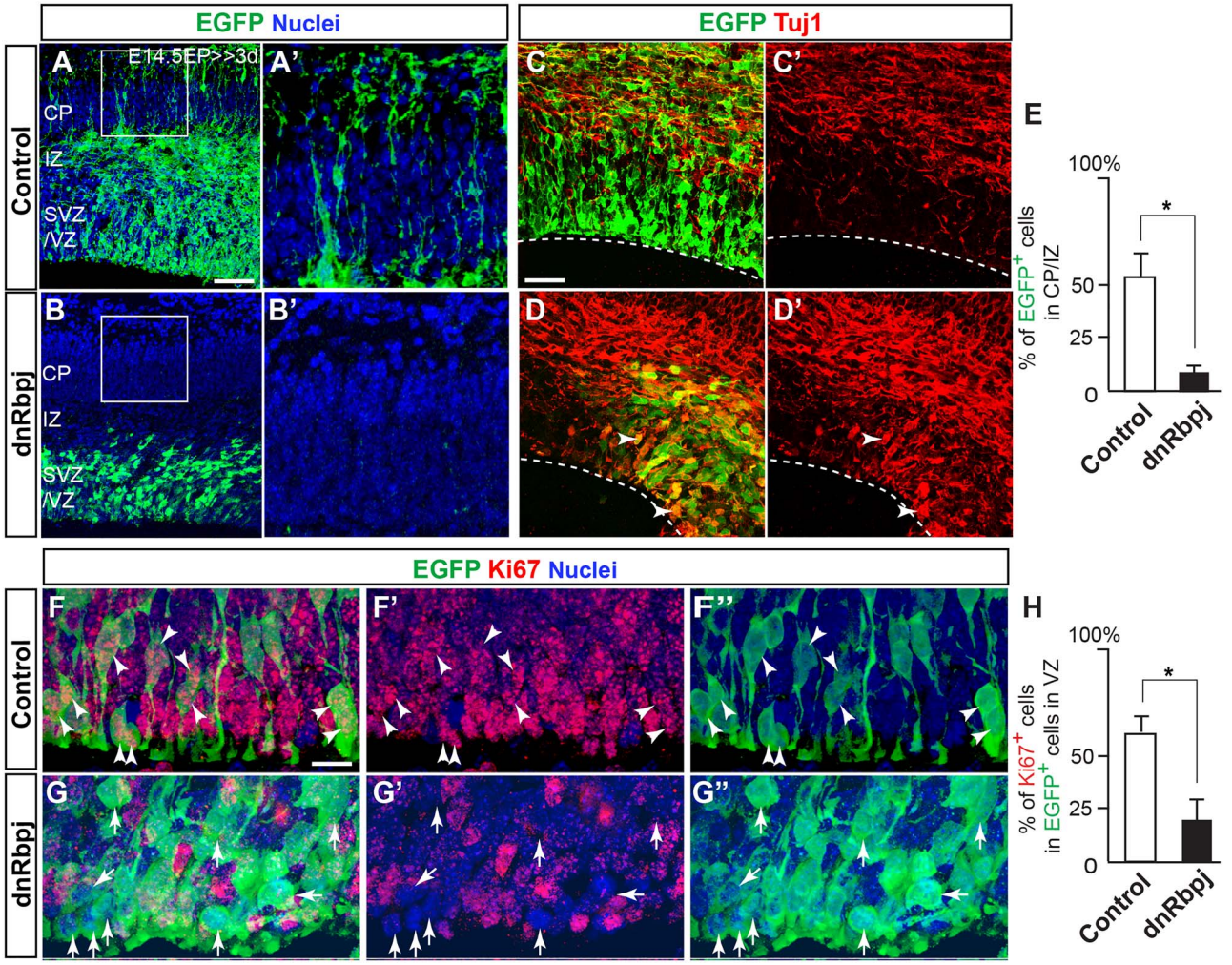

Figure 5. Expression of dnRbpj promotes neurogenesis. (*A–D′* and *F–G″*) EGFP immunostaining with Tuj1 (*C–D′*) or Ki67 (*F–G″*) 3 days after EP at E14.5 with dnRbpj (*B*, *B′*, *D*, *D′*, and *G–G″*) or control (empty pCMX) (*A*, *A′*, *C*, *C′*, and *F–F″*) plasmids. Nuclei were counterstained with DAPI. *A′* and *B′* are the higher magnification view of the squared areas in *A* and *B*, respectively. In the cortex electroporated with dnRbpj, EGFP$^+$ cells are found deeper in the cortex than those in the control-electroporaed cortex (compare *A* and *B*), and EGFP$^+$ radial glial fibers reaching to the pia were rarely observed (compare *A′* and *B′*). Many of dnRbpj-expressing cells in the VZ/SVZ are abnormally Tuj1$^+$ (arrowheads in *D* and *D′*, compare with *C* and *C′*) and Ki67$^-$ (arrows in *G–G″*, compare with *F–F″*). Bars (μm) = 100 (*A* and *B*), 25 (*C–D′*) and 10 (*F–G″*). (*E* and *H*) Quantification of the percentage of EGFP$^+$ cells in the IZ/CP (*E*), and that of Ki67$^+$ cells in EGFP$^+$ cells in the VZ (*H*), in the cortex electroporated with indicated plasmids. The data represent the mean ± SEM ($n = 5$ animals per condition). *$P < 0.01$ by Student's *t*-test.

2011) (pCMX-dnRbpj) with the pCAG-EGFP plasmid (for labeling of the electroporated cells) (Hashimoto-Torii et al. 2008) into the mouse cortex at E14.5 (Fig. 5, Supplementary Fig. 3). At E17.5, the majority of EGFP$^+$ dnRbpj-expressing cells were positioned deeper in the cortex than control cells (Fig. 5A, B, E). EGFP$^+$ radial glial fibers reaching to the pia were hardly detectable in dnRbpj electroporated brains (Fig. 5A′, B′), and consistently, many of these dnRbpj-expressing cells were Tuj1$^+$ (Fig. 5C–D′, see arrowheads in Fig. 5D, D′) and Ki67$^-$ (Fig. 5H, compare Fig. 5G–G″ with Fig. 5F–F″), indicating premature neuronal differentiation. dnRbpj-expressing cells also showed increased cell-cycle exit index (Supplementary Fig. 4). These results indicate that Rbpj is required for the maintenance of proliferative neural progenitor cells and inhibits neurogenesis, consistent with both the phenotypes observed in *Rbpj* cKO (Fig. 2) and previous reports on different stages or regions of the nervous system (Hitoshi et al. 2002; Gao et al. 2009; Imayoshi et al. 2010).

Rbpj is Required for Proper Radial Migration of Cortical Neurons

The activation of Rbpj in migrating neurons (Fig. 4), the positional defects of dnRbpj-introduced cells in the developing cortex (Fig. 5), and the abnormal distribution of cortical neuronal subtypes in *Rbpj* cKO mice (Figs 2 and 3) collectively suggest a role of Rbpj in neuronal migration. To dissociate the function of Rbpj specific in migrating neurons apart from its role in neural progenitor cells, we used the Cre/LoxP system to delete *Rbpj* specifically in migrating neurons (Fig. 6). We introduced pTα1-Cre-IRES-Venus, by which the α-tubulin promoter (Gloster et al. 1994) drives Cre recombinase only in neurons (Hashimoto-Torii et al. 2008), into the E14.5 cerebral cortex of floxed *Rbpj* mice by in utero EP and observed 6 days later. In comparison to the migration of Venus$^+$ neurons into upper cortical layers in control *Rbpj*$^{fl/+}$ electroporated mice, a significant number of Venus$^+$ neurons in *Rbpj*$^{fl/fl}$ mice were abnormally positioned in

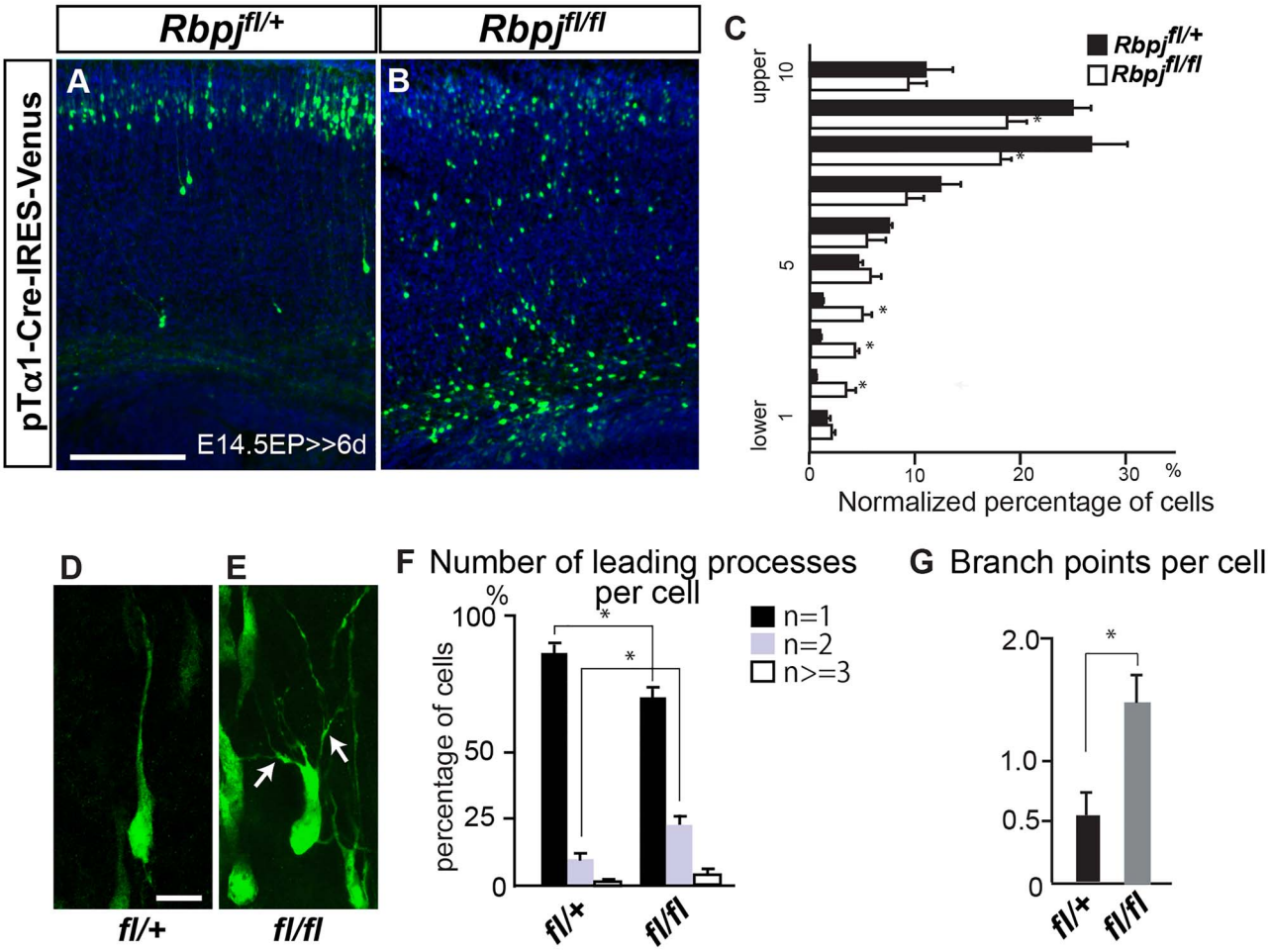

Figure 6. Neuron-specific *Rbpj* deletion causes radial migration defects and abnormal neuronal morphology during migration. (*A* and *B*) Venus immunostaining and nuclei labeling 6 days after EP at E14.5 with pTα1-Cre-IRES-Venus in $Rbpj^{fl/+}$ (*A*) and $Rbpj^{fl/fl}$ (*B*) mice, showing radial migration defects of neurons by deletion of *Rbpj*. Bar (μm) = 100. (*C*) Quantification of the distribution of $Venus^+$ neurons. $Venus^+$ neurons in $Rbpj^{fl/fl}$ mice were abnormally located in deeper layers comparing to those in $Rbpj^{fl/+}$ mice. The data represent the mean ± SEM ($n = 4$ animals per genotype). $P < 0.0001$ by Kolmogorov–Smirnov test. *$P < 0.05$ by Mann Whitney U pairwise comparisons between corresponding bins. (*D* and *E*) Venus immunostaining, revealing the morphology of migrating neurons 3 days post-EP with pTα1-Cre-IRES-Venus in the indicated mutants at E14.5. Arrows in E indicate ectopic processes of migrating neurons. Bar (μm) = 10. (*F* and *G*) Percentage of cells with one (black), two (gray) or > 3 (white) processes per cell (*F*), and the number of branch points per cell (branch points/primary processes) in $Venus^+$ neurons (*G*), showing an increase of the processes and branches in in $Rbpj^{fl/fl}$ mice comparing to those in $Rbpj^{fl/+}$ mice. The data represent the mean ± SEM ($n = 20$ cells from 5 brains per genotype). *$P < 0.05$ (*F*) and $P < 0.01$ (*G*) by Student's *t*-test.

deeper layers (Fig. 6A–C). In addition, morphological abnormalities of migrating neurons were commonly observed (Fig. 6D–G). In normal cortical development, newly generated neurons enter the multipolar stage, a temporal transitional state during which their processes become multifurcated within the subventricular zone (SVZ) through the IZ. Subsequently, the multipolar neurons assume a bipolar shape for further migration through the CP, extending one leading process toward the pial surface (LoTurco and Bai 2006). In contrast, *Rbpj*-deleted neurons exhibited abnormal morphology with multiple processes within the CP (Fig. 6E–G), suggesting that the multipolar-to-bipolar transition is affected or the leading processes of bipolar neurons are abnormally branched by *Rbpj* deletion. No effects of *Rbpj* deletion on apoptosis analyzed by Terminal deoxynucleotidyl transferase dUTP nick end labeling (TUNEL) staining in $Venus^+$ cells were observed (data not shown). Together, these results demonstrate a novel role of Rbpj in regulating proper morphological transition and radial migration of cortical neurons.

Context-Dependent Regulation of Ngn1 Expression by Rbpj

We next aimed to find the molecular target of Rbpj that mediates Rbpj's bifunctional role in neurogenesis and neuronal migration. A recent genome-wide analysis has provided a list of genes that are regulated by Notch-Rbpj signaling (Li et al. 2012). Among these genes, the upregulation of proneural factors such as neurogenins and mouse acute-scute homologues was shown in the neuroepithelium of caudal brain regions in *Rbpj* knockout mice at earlier developmental stages (Oka et al. 1995). Proneural basic helix-loop-helix genes including Neurogenins have also been shown to independently regulate both the neurogenic and cell migration machineries through the regulation of gene expression, activation, and inhibition by serving as molecular "linkers" connecting neurogenesis with migration (Hand et al. 2005; Ge et al. 2006). We therefore compared expression patterns of proneural genes with the pattern of Rbpj activity indicated

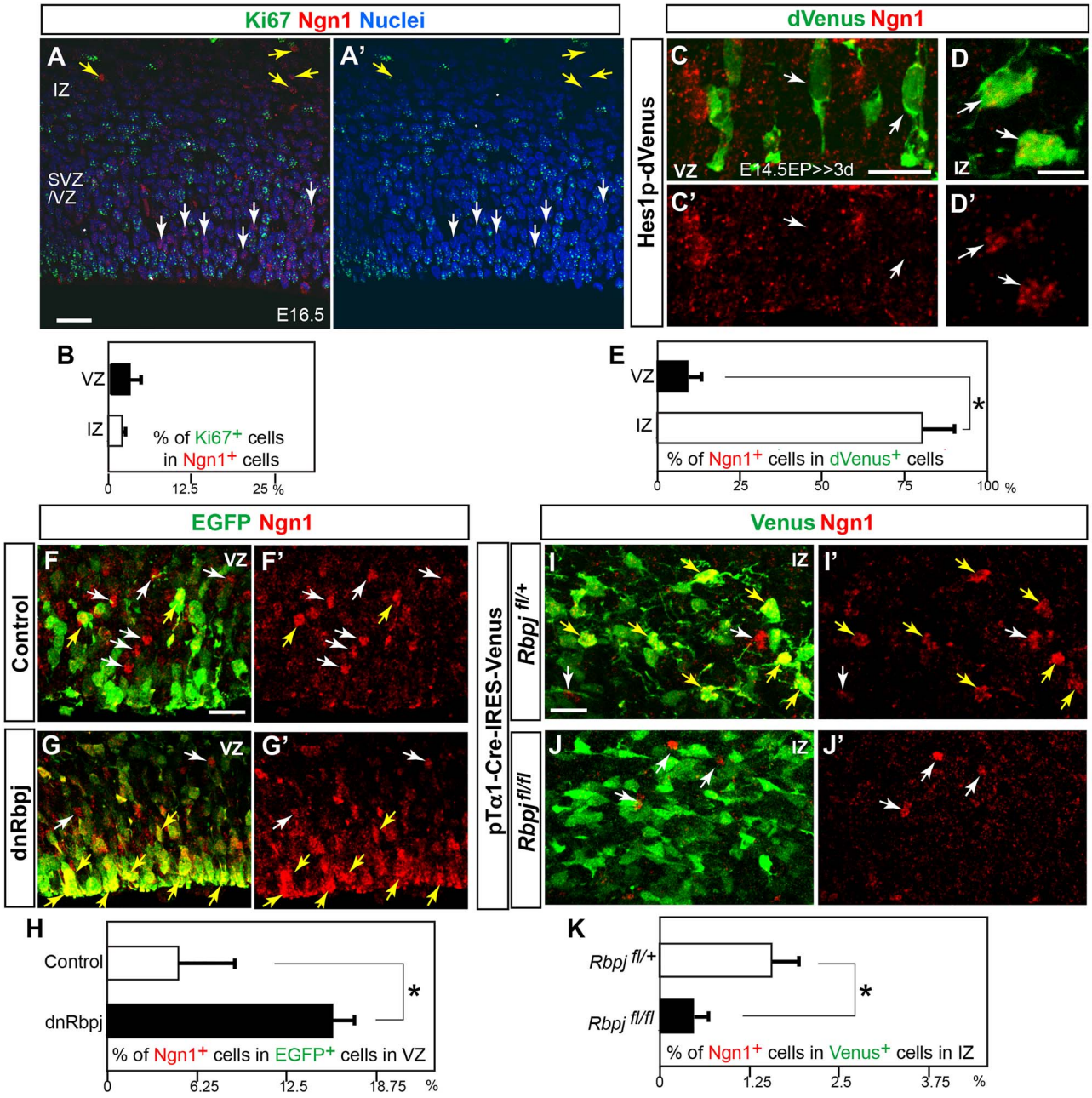

Figure 7. Differential regulation of Ngn1 by Rbpj in neural progenitor cells and migrating neurons. (*A* and *A*′) Immunostaining for Ki67 and Ngn1 in the cortex at E16.5, revealing that Ngn1$^+$ cells are not proliferative (i.e., Ki67$^-$). Nuclei are labeled with DAPI. Yellow and white arrows indicate Ngn1-expressing cells in the IZ and VZ/SVZ, respectively. Bar (μm) = 50. (*B*) Percentages of Ki67$^+$ cells in Ngn1$^+$ cells in the VZ and IZ. The data represent the mean ± SEM (n = 6 animals). (*C*–*D*′) Immunostaining for dVenus and Ngn1 in the VZ (*C* and *C*′) and IZ (*D* and *D*′) of the cortex 3 days after EP with Hes1p-dVenus at E14.5, showing that dVenus$^+$ cells are Ngn$^-$ in the VZ (arrows in *C* and *C*′) but Ngn$^+$ in the IZ (arrows in *D* and *D*′). Bars (μm) = 25 (*C* and *C*′) and 10 (*D* and *D*′). (*E*) Percentages of Ngn1$^+$ cells in dVenus$^+$ cells in the VZ and IZ in the cortex electroporated with Hes1p-dVenus. The data represent the mean ± SEM (n = 4 animals). *$P < 0.05$ by Mann-Whitney U test. (*F*–*G*′) Co-detection of EGFP and Ngn1 in the VZ 3 days after EP with the dnRbpj or control plasmid together with EGFP plasmid in wild-type mice. Yellow and white arrows indicate Ngn1$^+$ cells in EGFP$^+$ and EGFP$^-$ cells, respectively. Bar (μm) = 25. (*H*) Percentages of Ngn1$^+$ cells in EGFP$^+$ cells in the VZ as represented in *F*–*G*′. The data represent the mean ± SEM (n = 4 animals per condition). *$P < 0.05$ by Student's *t*-test. (*I*–*J*′) Co-detection of Venus and Ngn1 in the IZ 3 days after EP with the pTα1-Cre-IRES-Venus plasmid in *Rbpj*$^{fl/+}$ or *Rbpj*$^{fl/fl}$ mice. Yellow and white arrows indicate Ngn1$^+$ cells in Venus$^+$ and Venus$^-$ cells, respectively. Bar (μm) = 25. (*K*) Percentages of Ngn1$^+$ cells in Venus$^+$ cells in the IZ, as represented in *I*–*J*′. The data represent the mean ± SEM (n = 4 animals per genotype). *$P < 0.05$ by Student's *t*-test.

by dVenus under the control of Hes1 promoter (Hes1p-dVenus) (Fig. 7). Among the list, the expression of Ngn1, which is mainly observed in postmitotic neurons in the VZ/SVZ, showed a clear complementary pattern to that of dVenus (Fig. 7A–C′, E). However, to our surprise, Ngn1 is strongly colocalized with dVenus in neurons within the IZ (Fig. 7A and A′, D–E). To test Rbpj-mediated regulation of Ngn1 expression, we examined the effect of Rbpj suppression/deletion in neural progenitor cells and migrating neurons. Compared with the control EP (at E14.5 and observation 3 days later), the percentage of Ngn1$^+$ cells in the VZ

was increased in the neural progenitor cells electroporated with the dnRbpj expression construct (Fig. 7F–H). In stark contrast, the percentage of Ngn1$^+$ neurons in the IZ was significantly decreased by neuron-specific *Rbpj* deletion by EP with pTα1-Cre-IRES-Venus in *Rbpj*$^{f/f}$ mice (at E14.5 and observation 3 days later) (Fig. 7I–K). These results suggest that Rbpj negatively and positively controls Ngn1 expression in neural progenitor cells and migrating neurons, respectively, in the developing cerebral cortex.

Discussion

The present study shows the dual role of Rbpj in neurogenesis and neuronal migration (Supplementary Fig. 5). Our work has confirmed several previous reports, which have demonstrated that Rbpj is required for the maintenance of neural progenitor state by inhibiting neuronal differentiation (Imayoshi et al. 2010; Dave et al. 2011). Importantly, we found that this activity is critical not only for timely generation of proper numbers of layer-specific neuronal subtypes, but also for matching the balance between the numbers of radial glial scaffolds required for neuronal migration and the neurons to be generated. After the decrease in its expression for neuronal differentiation, Rbpj expression is restored in neurons, which is further required for their radial migration.

The Multifaceted Functions of Rbpj on Cortical Development

To circumvent embryonic lethality of conventional *Rbpj* knockout mice before the onset of neurogenesis, previous studies have explored the use of RNAi-mediated knockdown or cKO mouse approaches to address the role of Rbpj in cortical development in vivo. These studies have demonstrated that Rbpj-mediated Notch signaling is required for preventing neural progenitor cells to differentiate into neurogenic intermediate progenitors and neurons during embryonic cortical development (Mizutani et al. 2007; Imayoshi et al. 2010; Dave et al. 2011). Accelerated neurogenesis and premature depletion of cortical progenitor cells that we observed in our *Rbpj* cKO (*Emx1-Cre;Rbpj*$^{f/f}$) mice corroborate these previous findings.

Previously, our group and others have shown that the interaction between Notch and Reelin-Dab1 pathways is essential for the formation of radial glial scaffold (Keilani and Sugaya 2008; Sibbe et al. 2009), proper morphological changes of migrating neurons, and radial migration of neurons (Hashimoto-Torii et al. 2008). The present study indicates that Rbpj is critically involved in all of these processes, as the present in vivo data demonstrate that *Rbpj* cKO mice exhibit radial glial dysmorphology and abnormal neuronal invasion into layer I, both of which are similar to the *reeler* phenotype (Trommsdorff et al. 1999; Dulabon et al. 2000; Forster et al. 2002; Hartfuss et al. 2003; Hack et al. 2007). This provides further evidence for the critical involvement of Rbpj in several broad aspects of Notch and Reelin-mediated processes in cortical development. *Rbpj* cKO mice survive postnatally (until at least P50), which has enabled us to examine the impact of *Rbpj* deletion in cortical development through the postnatal period. The severe disruption of cortical organization in *Rbpj* cKO mice is likely due to the neuronal migration defects on top of the accelerated neurogenesis and premature depletion of radial glial scaffolds, as the phenotypes of other mutant mice that have either radial migration deficits such as *reeler* mice (Rice and Curran 2001; Forster et al. 2006) or accelerated neurogenesis (Ritchie et al. 2014; Yang et al. 2015) are not as severe as those observed in *Rbpj* cKO mice. Neurons generated at an abnormally accelerated rate may not have a sufficient number of radial glial scaffolds to advance apically as neural progenitor cells are prematurely depleted at the same time. Combined with the neuronal migration deficits, this may result in later-born neurons to crowd into the domains in which radial glial fibers are still available, hence generating an uneven distribution of these neurons along the tangential axis of the cortex.

Alternatively, although each layer-specific neuronal subtype appears to be generated across the cortex of *Rbpj* cKO mice despite at abnormal ratios (Fig. 3), some neural progenitor cells may generate only specific subtypes at local domains. This is possible if Rbpj plays a role in controlling the timely production of layer-specific neuronal subtypes. Interestingly, it has been suggested that mammals use a temporal sequence of the cortical neurogenetic program to generate a uniformly layered neocortex, whereas other amniotic species such as birds impose spatial constraints on the sequence to pattern the pallium (Suzuki et al. 2012; Nomura et al. 2014). In addition, the level of Rbpj-mediated canonical Notch signaling in pallial progenitor cells in these species is either higher or lower than that in mammalian cortical progenitors (Nomura et al. 2013) and may be applicable in here given the similarity between the nuclear organization of the pallium in non-mammalian amniotes and the abnormally clustered distribution of neuronal subtypes in the cortex of *Rbpj* cKO mice.

The Switching of Rbpj Transcriptional Activity in Cortical Developmental Contexts

A key feature that we found in the role of Rbpj in cortical development is the switching of its transcriptional activity during specific developmental phases; namely, Rpbj is turned off at neuronal differentiation and turned back on during radial migration. One potential mechanism is that the activated Notch (NICD), which interacts with Rbpj to induce its transcriptional activity for the maintenance of the neural progenitor state, is targeted for degradation by Fbxw7, an adaptor molecule of E3 ligase, upon neuronal differentiation (Hoeck et al. 2010; Matsumoto et al. 2011). This Fbxw7-mediated Notch degradation can then be suppressed in neurons during their migration by receiving the Reelin-Dab1 signaling (Hashimoto-Torii et al. 2008).

In addition, we also observed opposite regulations of Ngn1 by Rbpj in neural progenitor cells and migrating neurons. These activities are well coordinated with the function of Ngn1 during neurogenesis and neuronal migration (Ge et al. 2006). Whether Ngn1 is the primary mediator of Rbpj-dependent regulation of neuronal migration, and how Rbpj regulates Ngn1 in opposing effects within different cell types remains to be elucidated. During the progenitor cell stage, Rbpj has been shown to suppress proneural gene expression through the control of Hes transcription (Kageyama and Nakanishi 1997), consistent with our results in the VZ/SVZ. Recent studies have shown that specific co-factors such as Ptf1a with Rbpj can directly activate the transcription of Ngn2 in the spinal cord (Henke et al. 2009). Similar mechanisms may be involved in the stage-specific regulation of Ngn1 by Rbpj. As our approach of focusing on Rbpj, a downstream mediator of canonical Notch signaling has limitation in addressing specific roles of individual Notch 1–4 receptors, further studies in this direction would unravel in depth

the Rbpj-mediated mechanisms in the regulation of cortical development.

Supplementary Material

Supplementary material is available at *Cerebral Cortex* online.

Funding

National Institutes of Health, National Center for Advancing Translational Sciences (R00AA01838705, R01AA025215 and UL1TR000075 to K.H-T., R01MH111674 to M.T.); ABMRF/The Foundation for Alcohol Research (to K.H.-T.); Brain & Behavior Research Foundation, Scott-Gentle Foundation (to K.H-T. and M.T.); Avery Translational Research Career Development Program Award (to M.T.); District of Columbia Intellectual and Developmental Disabilities Research Center Award program (1U54HD090257-01).

Declaration

Its contents are solely the responsibility of the authors and do not necessarily represent the official views of the National Center for Advancing Translational Sciences or the National Institutes of Health. *Conflict of Interest*: None declared.

References

Ables JL, Breunig JJ, Eisch AJ, Rakic P. 2011. Not(ch) just development: notch signalling in the adult brain. *Nat Rev Neurosci*. 12:269–283.

Andersson ER, Sandberg R, Lendahl U. 2011. Notch signaling: simplicity in design, versatility in function. *Development*. 138:3593–3612.

Artavanis-Tsakonas S, Rand MD, Lake RJ. 1999. Notch signaling: cell fate control and signal integration in development. *Science*. 284:770–776.

Bray SJ. 2006. Notch signalling: a simple pathway becomes complex. *Nat Rev Mol Cell Biol*. 7:678–689.

Caviness VS Jr, Sidman RL. 1973. Time of origin or corresponding cell classes in the cerebral cortex of normal and reeler mutant mice: an autoradiographic analysis. *J Comp Neurol*. 148:141–151.

Chenn A, Walsh CA. 2002. Regulation of cerebral cortical size by control of cell cycle exit in neural precursors. *Science*. 297:365–369.

Corbin JG, Nery S, Fishell G. 2001. Telencephalic cells take a tangent: non-radial migration in the mammalian forebrain. *Nat Neurosci*. 4(Suppl):1177–1182.

Dave RK, Ellis T, Toumpas MC, Robson JP, Julian E, Adolphe C, Bartlett PF, Cooper HM, Reynolds BA, Wainwright BJ. 2011. Sonic hedgehog and notch signaling can cooperate to regulate neurogenic divisions of neocortical progenitors. *PLoS One*. 6:e14680.

Dulabon L, Olson EC, Taglienti MG, Eisenhuth S, McGrath B, Walsh CA, Kreidberg JA, Anton ES. 2000. Reelin binds alpha3beta1 integrin and inhibits neuronal migration. *Neuron*. 27:33–44.

Fishell G, Kriegstein A. 2005. Cortical development: new concepts. *Neuron*. 46:361–362.

Forster E, Jossin Y, Zhao S, Chai X, Frotscher M, Goffinet AM. 2006. Recent progress in understanding the role of Reelin in radial neuronal migration, with specific emphasis on the dentate gyrus. *Eur J Neurosci*. 23:901–909.

Forster E, Tielsch A, Saum B, Weiss KH, Johanssen C, Graus-Porta D, Muller U, Frotscher M. 2002. Reelin, disabled 1, and beta 1 integrins are required for the formation of the radial glial scaffold in the hippocampus. *Proc Natl Acad Sci U S A*. 99:13178–13183.

Gao F, Zhang Q, Zheng MH, Liu HL, Hu YY, Zhang P, Zhang ZP, Qin HY, Feng L, Wang L, et al. 2009. Transcription factor RBP-J-mediated signaling represses the differentiation of neural stem cells into intermediate neural progenitors. *Mol Cell Neurosci*. 40:442–450.

Ge W, He F, Kim KJ, Blanchi B, Coskun V, Nguyen L, Wu X, Zhao J, Heng JI, Martinowich K, et al. 2006. Coupling of cell migration with neurogenesis by proneural bHLH factors. *Proc Natl Acad Sci U S A*. 103:1319–1324.

Giniger E. 2012. Notch signaling and neural connectivity. *Curr Opin Genet Dev*. 22:339–346.

Gloster A, Wu W, Speelman A, Weiss S, Causing C, Pozniak C, Reynolds B, Chang E, Toma JG, Miller FD. 1994. The T alpha 1 alpha-tubulin promoter specifies gene expression as a function of neuronal growth and regeneration in transgenic mice. *J Neurosci Official J Soc Neurosci*. 14:7319–7330.

Hack I, Hellwig S, Junghans D, Brunne B, Bock HH, Zhao S, Frotscher M. 2007. Divergent roles of ApoER2 and Vldlr in the migration of cortical neurons. *Development*. 134:3883–3891.

Han H, Tanigaki K, Yamamoto N, Kuroda K, Yoshimoto M, Nakahata T, Ikuta K, Honjo T. 2002. Inducible gene knockout of transcription factor recombination signal binding protein-J reveals its essential role in T versus B lineage decision. *Int Immunol*. 14:637–645.

Hand R, Bortone D, Mattar P, Nguyen L, Heng JI, Guerrier S, Boutt E, Peters E, Barnes AP, Parras C, et al. 2005. Phosphorylation of Neurogenin2 specifies the migration properties and the dendritic morphology of pyramidal neurons in the neocortex. *Neuron*. 48:45–62.

Hartfuss E, Forster E, Bock HH, Hack MA, Leprince P, Luque JM, Herz J, Frotscher M, Gotz M. 2003. Reelin signaling directly affects radial glia morphology and biochemical maturation. *Development*. 130:4597–4609.

Hashimoto-Torii K, Motoyama J, Hui CC, Kuroiwa A, Nakafuku M, Shimamura K. 2003. Differential activities of sonic hedgehog mediated by Gli transcription factors define distinct neuronal subtypes in the dorsal thalamus. *Mech Dev*. 120:1097–1111.

Hashimoto-Torii K, Torii M, Sarkisian MR, Bartley CM, Shen J, Radtke F, Gridley T, Sestan N, Rakic P. 2008. Interaction between Reelin and notch signaling regulates neuronal migration in the cerebral cortex. *Neuron*. 60:273–284.

Henke RM, Savage TK, Meredith DM, Glasgow SM, Hori K, Dumas J, MacDonald RJ, Johnson JE. 2009. Neurog2 is a direct downstream target of the Ptf1a-Rbpj transcription complex in dorsal spinal cord. *Development*. 136:2945–2954.

Hitoshi S, Alexson T, Tropepe V, Donoviel D, Elia AJ, Nye JS, Conlon RA, Mak TW, Bernstein A, van der Kooy D. 2002. Notch pathway molecules are essential for the maintenance, but not the generation, of mammalian neural stem cells. *Genes Dev*. 16:846–858.

Hoeck JD, Jandke A, Blake SM, Nye E, Spencer-Dene B, Brandner S, Behrens A. 2010. Fbw7 controls neural stem cell differentiation and progenitor apoptosis via notch and c-Jun. *Nat Neurosci*. 13:1365–1372.

Imayoshi I, Kageyama R. 2011. The role of notch signaling in adult neurogenesis. *Mol Neurobiol*. 44:7–12.

Imayoshi I, Sakamoto M, Yamaguchi M, Mori K, Kageyama R. 2010. Essential roles of notch signaling in maintenance of neural stem cells in developing and adult brains. *J Neurosci Offic J Soc Neurosci*. 30:3489–3498.

Kageyama R, Nakanishi S. 1997. Helix-loop-helix factors in growth and differentiation of the vertebrate nervous system. *Curr Opin Genet Dev*. 7:659–665.

Kato H, Taniguchi Y, Kurooka H, Minoguchi S, Sakai T, Nomura-Okazaki S, Tamura K, Honjo T. 1997. Involvement of RBP-J in biological functions of mouse Notch1 and its derivatives. *Development*. 124:4133–4141.

Keilani S, Healey D, Sugaya K. 2012. Reelin regulates differentiation of neural stem cells by activation of notch signaling through Disabled-1 tyrosine phosphorylation. *Can J Physiol Pharmacol*. 90:361–369.

Keilani S, Sugaya K. 2008. Reelin induces a radial glial phenotype in human neural progenitor cells by activation of Notch-1. *BMC Dev Biol*. 8:69.

Kohyama J, Tokunaga A, Fujita Y, Miyoshi H, Nagai T, Miyawaki A, Nakao K, Matsuzaki Y, Okano H. 2005. Visualization of spatiotemporal activation of notch signaling: live monitoring and significance in neural development. *Dev Biol*. 286:311–325.

Kolk SM, de Mooij-Malsen AJ, Martens GJ. 2011. Spatiotemporal molecular approach of in utero electroporation to functionally decipher Endophenotypes in neurodevelopmental disorders. *Front Mol Neurosci*. 4:37.

Komine O, Nagaoka M, Watase K, Gutmann DH, Tanigaki K, Honjo T, Radtke F, Saito T, Chiba S, Tanaka K. 2007. The monolayer formation of Bergmann glial cells is regulated by notch/RBP-J signaling. *Dev Biol*. 311:238–250.

Li X, Zhao X, Fang Y, Jiang X, Duong T, Fan C, Huang CC, Kain SR. 1998. Generation of destabilized green fluorescent protein as a transcription reporter. *J Biol Chem*. 273:34970–34975.

Li Y, Hibbs MA, Gard AL, Shylo NA, Yun K. 2012. Genome-wide analysis of N1ICD/RBPJ targets in vivo reveals direct transcriptional regulation of Wnt, SHH, and hippo pathway effectors by Notch1. *Stem Cells*. 30:741–752.

Liu S, Wang Y, Worley PF, Mattson MP, Gaiano N. 2015. The canonical notch pathway effector RBP-J regulates neuronal plasticity and expression of GABA transporters in hippocampal networks. *Hippocampus*. 25:670–678.

LoTurco JJ, Bai J. 2006. The multipolar stage and disruptions in neuronal migration. *Trends Neurosci*. 29:407–413.

Louvi A, Artavanis-Tsakonas S. 2006. Notch signalling in vertebrate neural development. *Nat Rev Neurosci*. 7:93–102.

Mason HA, Rakowiecki SM, Gridley T, Fishell G. 2006. Loss of notch activity in the developing central nervous system leads to increased cell death. *Dev Neurosci*. 28:49–57.

Matsumoto A, Onoyama I, Sunabori T, Kageyama R, Okano H, Nakayama KI. 2011. Fbxw7-dependent degradation of notch is required for control of "stemness" and neuronal-glial differentiation in neural stem cells. *J Biol Chem*. 286: 13754–13764.

Mizutani K, Yoon K, Dang L, Tokunaga A, Gaiano N. 2007. Differential notch signalling distinguishes neural stem cells from intermediate progenitors. *Nature*. 449:351–355.

Mumm JS, Kopan R. 2000. Notch signaling: from the outside in. *Dev Biol*. 228:151–165.

Nakhai H, Siveke JT, Klein B, Mendoza-Torres L, Mazur PK, Algul H, Radtke F, Strobl L, Zimber-Strobl U, Schmid RM. 2008. Conditional ablation of notch signaling in pancreatic development. *Development*. 135:2757–2765.

Nomura T, Gotoh H, Ono K. 2013. Changes in the regulation of cortical neurogenesis contribute to encephalization during amniote brain evolution. *Nat Commun*. 4:2206.

Nomura T, Murakami Y, Gotoh H, Ono K. 2014. Reconstruction of ancestral brains: exploring the evolutionary process of encephalization in amniotes. *Neurosci Res*. 86:25–36.

Oka C, Nakano T, Wakeham A, de la Pompa JL, Mori C, Sakai T, Okazaki S, Kawaichi M, Shiota K, Mak TW, et al. 1995. Disruption of the mouse RBP-J kappa gene results in early embryonic death. *Development*. 121:3291–3301.

Pierfelice T, Alberi L, Gaiano N. 2011. Notch in the vertebrate nervous system: an old dog with new tricks. *Neuron*. 69:840–855.

Rakic P. 2003. Developmental and evolutionary adaptations of cortical radial glia. *Cereb Cortex*. 13:541–549.

Rakic P. 2007. The radial edifice of cortical architecture: from neuronal silhouettes to genetic engineering. *Brain Res Rev*. 55:204–219.

Redmond L, Oh SR, Hicks C, Weinmaster G, Ghosh A. 2000. Nuclear Notch1 signaling and the regulation of dendritic development. *Nat Neurosci*. 3:30–40.

Rice DS, Curran T. 2001. Role of the reelin signaling pathway in central nervous system development. *Annu Rev Neurosci*. 24:1005–1039.

Ritchie K, Watson LA, Davidson B, Jiang Y, Berube NG. 2014. ATRX is required for maintenance of the neuroprogenitor cell pool in the embryonic mouse brain. *Biology Open*. 3: 1158–1163.

Rubenstein JL, Rakic P. 1999. Genetic control of cortical development. *Cereb Cortex*. 9:521–523.

Sanada K, Tsai LH. 2005. G protein betagamma subunits and AGS3 control spindle orientation and asymmetric cell fate of cerebral cortical progenitors. *Cell*. 122:119–131.

Sestan N, Artavanis-Tsakonas S, Rakic P. 1999. Contact-dependent inhibition of cortical neurite growth mediated by notch signaling. *Science*. 286:741–746.

Sibbe M, Forster E, Basak O, Taylor V, Frotscher M. 2009. Reelin and Notch1 cooperate in the development of the dentate gyrus. *J Neurosci*. 29:8578–8585.

Suzuki IK, Kawasaki T, Gojobori T, Hirata T. 2012. The temporal sequence of the mammalian neocortical neurogenetic program drives mediolateral pattern in the chick pallium. *Dev Cell*. 22:863–870.

Tanigaki K, Han H, Yamamoto N, Tashiro K, Ikegawa M, Kuroda K, Suzuki A, Nakano T, Honjo T. 2002. Notch-RBP-J signaling is involved in cell fate determination of marginal zone B cells. *Nat Immunol*. 3:443–450.

Taylor MK, Yeager K, Morrison SJ. 2007. Physiological notch signaling promotes gliogenesis in the developing peripheral and central nervous systems. *Development*. 134: 2435–2447.

Torii M, Hashimoto-Torii K, Levitt P, Rakic P. 2009. Integration of neuronal clones in the radial cortical columns by EphA and ephrin-A signalling. *Nature*. 461:524–528.

Torii M, Levitt P. 2005. Dissociation of corticothalamic and thalamocortical axon targeting by an EphA7-mediated mechanism. *Neuron*. 48:563–575.

Trommsdorff M, Gotthardt M, Hiesberger T, Shelton J, Stockinger W, Nimpf J, Hammer RE, Richardson JA, Herz J. 1999. Reeler/disabled-like disruption of neuronal migration in knockout mice lacking the VLDL receptor and ApoE receptor 2. *Cell*. 97:689–701.

Yang M, Yang SL, Herrlinger S, Liang C, Dzieciatkowska M, Hansen KC, Desai R, Nagy A, Niswander L, Moss EG, et al. 2015.

Lin28 promotes the proliferative capacity of neural progenitor cells in brain development. *Development*. 142:1616–1627.

Yang X, Klein R, Tian X, Cheng HT, Kopan R, Shen J. 2004. Notch activation induces apoptosis in neural progenitor cells through a p53-dependent pathway. *Dev Biol*. 269:81–94.

Zhu X, Zhang J, Tollkuhn J, Ohsawa R, Bresnick EH, Guillemot F, Kageyama R, Rosenfeld MG. 2006. Sustained notch signaling in progenitors is required for sequential emergence of distinct cell lineages during organogenesis. *Genes Dev*. 20:2739–2753.